Mutual Diffusion in PMMA/PnBMA Copolymer Films: Influence of the Solvent-Induced Glass Transition

Anne-Claire Dubreuil, Frédéric Doumenc, Béatrice Guerrier, Catherine Allain

Mutual diffusion in PMMA/PnBMA copolymer films: Influence of the solvent-induced glass transition

Anne-Claire Dubreuil, Frédéric Doumenc, Béatrice Guerrier[1], Catherine Allain

Lab. FAST (Université Pierre et Marie Curie - Université Paris Sud - CNRS)
Bât. 502, Campus Universitaire, 91405 Orsay, France

Abstract: In the framework of solvent diffusion in glassy polymer films this paper concerns an experimental study of sorption and desorption kinetics for a model system consisting of statistical PMMA/PnBMA copolymer films of various composition. The experimental results are obtained by performing differential increasing and decreasing pressure steps, using a gravimetric technique based on a quartz crystal microbalance placed in a controlled solvent vapor pressure chamber. The non-Fickian behavior in the glassy state and the variations of the mutual diffusion coefficient with the solvent concentration on one hand and with the copolymer composition on the other hand are studied. Results are analyzed in terms of absolute solvent mass fraction (ω_S) and in terms of distance to the glass transition ($\omega_S - \omega_{Sg}$). This last representation highlights the prevailing part of the gap to the glass transition in the system under study.

[1]Corresponding author; E-mail: guerrier@fast.u-psud.fr; Fax: +33 1 69 15 80 60; Tel: +33 1 69 15 80 63

1 Introduction

The behavior of polymers in the glassy state is complex and several theoretical approaches attempt to explain the structure and the dynamics of glassy materials. Most of the works on glass transition concern the temperature induced glass transition: starting from a high temperature where the polymer is rubbery, the sample is cooled down and enters the glassy state. Due to the dynamic nature of the glass transition the structure of glassy materials depends on the sample history, and various experimental studies concern the influence of the cooling rate on the glass transition temperature and the physical aging effects. Another way to go through the glass transition which is much less documented is to use the solvent concentration of the polymer solution as control parameter: starting from a dilute state, the polymer solution is dried up to the pure polymer. If the temperature of the experiment is below the glass transition temperature of the pure polymer, the solution goes through the glass transition for a given solvent concentration. In this paper only thick films are considered, so that no film thickness dependence is expected. The solvent induced glass transition is of great importance for practical applications since most of polymer coatings are obtained by drying polymer/solvent solutions.

To investigate diffusion in concentrated solutions, gravimetric methods are particularly suitable: indeed, the evolution of the mass of a film in response to an imposed step of solvent vapor pressure allows to analyze the swelling or drying kinetics and to determine the mutual diffusion coefficient. However, near the glass transition the coupling between diffusion and viscoelastic relaxation leads to complex kinetics for the film mass evolution. In the glassy domain, the film is thermodynamically out of equilibrium and the relaxation of the stresses induced by volume variations involves slow rearrangements of the macromolecular chains. When the time scales characterizing diffusion and relaxation are comparable, it is well known that the film mass evolution during swelling or drying is no more Fickian. Although numerous works have been devoted to this problem [1, 2, 3, 4, 5, 6, 7, 8], the involved phenomena are not yet completely understood. Experimental investigations of the mutual diffusion coefficient in the glassy domain have been performed for a few systems only and they show rather contradictory conclusions about the influence of the glass transition. In some cases, the variation of the mutual diffusion coefficient with the polymer concentration exhibits no dramatic anomaly when crossing the glass transition: a large decrease when polymer concentration increases is still observed, as described by the

classical free volume model in the rubbery state [9]. In other cases a change in the behavior is observed when the polymer concentration becomes greater than the value corresponding to the glass transition: the diffusion coefficient remains nearly constant or decreases much slower than in the previous case [3, 10].

In the present work we have studied the influence of the glass transition on the mutual diffusion for a model system composed of a family of statistical PMMA/PnBMA copolymers of various composition. Copolymer thick films (220nm to 1000nm) are swelled and deswelled by controlling the solvent (toluene) vapor pressure, allowing measurements for different solvent concentrations in particular in the glassy domain. A previous paper was dedicated to the characterization of solvent induced glass transition for the two homopolymers PMMA and PnBMA and four copolymers [11]. The pure copolymer glass transition temperatures vary monotonously with their compositions, from 131^oC (pure PMMA) to 34^oC (pure PnBMA). By performing a slow decreasing solvent pressure ramp at constant temperature (25^oC), that is a progressive drying from a very swollen state to the dry copolymer, the solvent mass fraction at the glass transition was shown to vary from 0.19 for PMMA to 0.02 for PnBMA: so the copolymers samples rich in PMMA

clearly undergo the glass transition during the drying while the copolymers samples rich in PnBMA remain rubbery except at the very end of drying. This paper reports the study of sorption and desorption kinetics for the same set of copolymers at various solvent concentrations in order to characterize the non-Fickian behavior in the glassy state, and the variations of the polymer/solvent mutual diffusion coefficient with the solvent concentration on one hand and with the copolymer composition on the other hand. Results are analyzed in terms of absolute solvent mass fraction (ω_S) and in term of distance to the glass transition ($\omega_S - \omega_{Sg}$) by analogy to temperature investigations.

The paper is organized as follows: A brief description of synthesis and characterization of the polymers, sample preparation, experimental setup and procedure are given in section 2. Section 3 is devoted to the qualitative analysis of the kinetics. The time dependent solubility model and the set inversion method used to analyze the data are presented in section 4. The quantitative analysis of the experimental kinetics as well as the behavior of the mutual diffusion coefficients and relaxation times are then detailed and compared to other experimental works.

2 Experimental

2.1 Materials and sample preparation

The polymer samples used in this study were kindly prepared by T. Wagner and T. Stoehr (Max Planck Institute for Polymer Research, Mainz, Germany). Synthesis and characterization have been described in [11] and we only recall the main results. Copolymer compositions and tacticities were measured by ^{1}H-NMR and ^{13}C-NMR in $CDCl_3$ on 300-MHz and 75-MHz Brucker AC-300 spectrometers. Molecular weights and polydispersities were determined by GPC, relative to PMMA standard, using a Waters apparatus. The glass transition temperatures Tg_0 ("midpoint" temperatures) and the specific heat variation at the glass transition ΔCpp were investigated by means of a Mettler DSC-30 differential scanning calorimeter. The heating rate was $10^0 C/$min. Molecular characteristics and calorimetric data are summarized in Table 1. The rather high glass transition temperatures of PMMA and PnBMA are typical values for syndiotactic-rich PMMA and PnBMA [12, 13]. The copolymer glass transition temperatures vary monotonously with their compositions as reported by Penzel et al. [14]. Toluene (Riedel-de Haën GmbH) was used as solvent for sorption and desorption experiments.

The polymer films were spin-cast directly onto the gold electrode of

piezoelectric quartz crystals. Their thicknesses were chosen in the range $200nm - 1\mu m$, to obtain rapid diffusion as well as accurate determination of solvent mass fraction [15].

2.2 Experimental set-up and procedure

2.2.1 Experimental setup

A detailed description of the experimental setup has been given elsewhere [16, 15]. The polymer film cast onto a quartz crystal resonator is located inside a vacuum chamber that is connected through electronic valves to a solvent reservoir (in which the solvent vapor pressure is equal to the saturated vapor pressure of pure solvent, ie. $P_{vs0} = 28.4$ Torr at $T = 25^oC$ for toluene), to a vacuum pump and to a secondary vacuum chamber. The lowest pressure reached under continuous pumping is 10^{-3} Torr. Since the experiments are undertaken at much larger pressures, this state is called "zero pressure" in the following. The pressure in the chamber is controlled by a PID regulation, allowing to maintain the pressure constant for several hours. Rapid pressure steps are possible by opening a valve connecting the sample compartment to a secondary chamber. Depending on the pressure difference between the two chambers, the step amplitude is between 0.5 and 2 Torr for sorption and between 0.2 and 1 Torr for desorption. The two chambers

allow for very reproducible and well defined differential steps (small activity steps). Note that, as there is no inert gas in the chamber, the pressure in the chamber corresponds to the vapor pressure of solvent. Using a thermostat, the chamber temperature is adjusted to T = 25 ± 0.15 ^{o}C.

2.2.2 Mass determination

The mass determination is detailed in [17]. When a thin film is cast onto one of the electrodes of a thickness-shear resonator, its acoustical resonance frequencies change due to the mass of the film. The film mass is deduced from the shift of the resonance frequency of one ("linear mass") or several ("cubic mass") harmonics. The first methods use the conductance curve to estimate the frequency shift. The mass determination takes about 5 seconds per data point when using the "linear mass" and 30 seconds when using the "cubic mass" with 6 harmonics. Another procedure is based on the analysis of the susceptance spectrum [16]. The time for data acquisition is then decreased to about 0.2 second.

Because of the long duration of the experiments performed (typically several hours), the performance of quartz microbalance (monolayer sensitivity) is affected by various phenomena. The evaluation of the corresponding uncertainties are detailed in [15, 17] and we just recall the main results used in

the quantitative estimation of diffusion coefficients.

First, resonance frequencies of a quartz depend on temperature [18]. In the vacuum ($P = 10^{-3}$ Torr) and around 25 ^oC, preliminary measurements on several blank quartz plates give an estimation of the maximum corresponding sensitivity of $-10^{-6}\, kg/m^2/^oC$. Resonance frequencies of a quartz also depend on pressure [18]. Preliminary experiments on blank quartz in toluene vapor showed that the systematic error due to pressure effects increases as pressure increases from $10^{-7} kg/m^2/Torr$ below 9 Torr to 2.5 $10^{-6} kg/m^2/Torr$ at 28 Torr. Another uncertainty comes from the limitation of the validity domain of the theoretical models of quartz microbalances: differences have been observed between "linear mass" and "cubic mass" (cf for example figure 1b), and between the "susceptance" method and "conductance method" [17].

Given the very small solvent uptakes envolved in the experiments performed in this study, these various systematic errors are significant and a specific estimation method appropriated to non random errors has been used to analyze the experimental data (cf section 4.2).

2.2.3 Experimental procedure

In the glassy domain viscoelastic relaxation involves characteristic times of the same order as the experiment durations and the film does not reach equilibrium. As a consequence, the results depend on the entire film history and the whole procedure must be carefully defined. In most of differential sorption or desorption experiments reported in the literature, pressure steps are performed one after the other, like "stairs". We have chosen another experimental procedure: before each increasing step, the film is kept at high pressure (about 25 Torr) for about two hours. The film is then largely swollen and in the rubbery state, allowing the whole previous story to be "forgotten". Starting from this well defined rubbery state, the pressure is lowered to the initial pressure chosen for the sorption step. This initial pressure is maintained a few hours until a "quasi-equilibrium" is reached (i.e. solvent diffusion is achieved and mass change due to relaxation is very small). Then the differential increasing pressure step is performed and the final pressure maintained for about 5 to 10 hours. Afterwards a decreasing step of about the same amplitude is performed. With such a protocol, the film history in the glassy state before each step is limited to a sharp decrease of the activity followed by a known waiting time. The sample is then in an expanded state

compared for example to an annealed sample. As shown in previous studies the sorption rates of films may differ with the sample history [1, 2, 8]. A more detailed study of the influence of the experimental protocol and film preparation, and thence of the state of the film, on the mutual diffusion coefficient is beyond the scope of this paper.

3 Qualitative analysis of the kinetics

Deviation from fickian kinetics in the glassy state was observed by several authors when performing sorption or desorption experiments, due to the coupling between solvent diffusion through the film and polymer matrix relaxation. Qualitative description of these non-fickian kinetics highlights various behaviors (sigmoïd, pseudo-fickian, two steps, case II,...) depending on the experiment performed (sorption or desorption, differential or large pressure steps), the studied systems and the experimental procedure [2, 3, 4, 5, 6, 7, 8].

An example of typical kinetics obtained in our experiments is given in figure 1 for the copolymer 84/16. The abscissa is $t^{1/2}/e$. The ordinate is $\frac{\omega_s - \omega_{si}}{\Delta a}$, where ω_s is the solvent mass fraction and ω_{si} its initial value. Δa is the imposed activity change during the step ($\Delta a = \Delta P / P_{VS0}$). This coordinate allows the comparison of steps having slightly different pressure amplitudes, and the comparison of sorption and desorption steps. In this representation,

Fickian kinetics corresponds to a linear increase at short times and to the saturation toward an asymptotic value at large times.

As expected for the experiments performed at a low pressure corresponding to the glassy domain, the kinetics curve are clearly non-fickian and close to the so-called pseudo-fickian kinetics, which exhibits a linear part at short times followed by a slow increase of $\frac{\omega_s - \omega_{si}}{\Delta a}$. Most of the performed experiments exhibit the same behavior and, contrary to some authors, no S shape or two stages curves were observed whatever the pressure. All the kinetics show a good reproducibility (Figure 1a-1d), except for the steps from and towards 0 Torr (Figure 1e). The kinetics obtained just after annealing differ from the one obtained by the experimental procedure described above, as already observed on glassy polymers [1]. Besides this phenomenon due to a different initial state (annealed films are very compacted), the reproducibility between the kinetics obtained for quite similar film histories is also poor. These odd behaviors at 0 Torr are still not understood despite various explanations can be suggested. The assumption of linearity (differential steps involving a constant diffusion coefficient) may be erroneous since the diffusion coefficient could decrease very strongly near 0 Torr, i.e. when solvent concentration goes to zero. The lowest pressure (called "0 Torr") is not ac-

curately measured and is about 10^{-3} Torr. Some authors put forward the development of longitudinal stresses in the viscoelastic film [4]. Given the un-understood behavior of the sorption or desorption steps from or towards 0 Torr, we do not take these data into account in the study of the diffusion coefficient.

Finally let us note that in the range of accuracy of our measurements, sorption and desorption kinetics are similar at least at short times when diffusion is dominating. This also confirms the assumption of differential steps. The difference that appears at the end of the measurement may come from either external effects (temperature drift for example) or from intrinsic phenomena: indeed, the film being out of equilibrium in the glassy state, with a large distribution of relaxation times, the long time behavior depends in a complex manner on the thermal and mechanical history of the film, or the use of free or supported films [2, 8]. Experimental data are actually not sufficient to go further in the interpretation of long time behaviors.

4 Quantitative analysis

4.1 Time dependent solubility model

Several theoretical approaches have been proposed, none of them succeeding in fitting all the non-fickian kinetics [19]. One of these approaches takes viscoelastic relaxation into account through a constitutive equation, where the viscoelastic behavior is approximated by a Maxwell model [20, 21, 22, 23]. A second approach takes the coupling between diffusion and relaxation into account through the solubility (time dependent solubility model [24, 25, 26, 27, 28, 9]). In this paper, the change in solubility is only expressed through a time variable boundary condition at the film/vapor interface [24], with:

$$c(z = e, t > 0) \; = \; c_0 + (c_\infty - c_0) \left[1 - exp \left(- \frac{t}{\tau_r} \right) \right] \tag{1}$$

where e is the film thickness, c_0 the instantaneous change in surface concentration, c_∞ the equilibrium concentration and τ_r the relaxation characteristic time. No new driving term appears in the equation describing solvent transport inside the film which is expressed by the Fick equation (with a constant mutual diffusion coefficient as only differential pressure steps are considered):

$$\partial c(z,t)/\partial t = D_{SP} \;\; \partial^2 c(z,t)/\partial z^2, \quad 0 < z < e \tag{2}$$

The only change compared to the model used to fit classical fickian kinetics comes from the variation of solubility induced by the time-dependent boundary condition. This simple model is known to allow the description of the different types of kinetics and fits very well our data. It yields to an analytical final result and involves four parameters, c_0 and c_∞ for solubility, $\tau_d = e^2/D_{SP}$ and τ_r for the characteristic times of diffusion and relaxation respectively. The mass increase due to a differential pressure step is:

$$\begin{aligned} \Delta m^*(t) \;=\; 1 - tan\left(\frac{1}{\sqrt{deb}}\right)\sqrt{deb}\;(1-R)\;exp\left(-\frac{t^*}{deb}\right) \\ +\;2\sum_{k'=\frac{\pi}{2}}^{\infty}\;\frac{\frac{1}{deb}-Rk'^2}{k'^2\left(k'^2-\frac{1}{deb}\right)}\;exp\left\{-k'^2t^*\right\} \end{aligned} \tag{3}$$

with

$$\Delta m^*(t) = \frac{(m(t)-m_i)}{(m_\infty - m_i)} \qquad , \qquad t^{*\frac{1}{2}} = \frac{\sqrt{D_{sp}t}}{e} = \sqrt{\frac{t}{\tau_d}}$$

and with $k^{'} = (2k+1)\frac{\pi}{2}$, $deb = \tau_r/\tau_d$ (the Deborah number), $R = (c_0 - c_i)/(c_\infty - c_i)$. c_i is the initial concentration and m_i the initial mass.

Let us note that many macromolecular modes are involved during polymer matrix relaxation so that taking the relaxation into account through a first order model is a rough approximation. In a previous study, we have extended the solubility model introducing a relaxation time distribution (stretched

exponential model). It was shown that these two descriptions of relaxation lead to about the same estimates of the diffusion coefficient [15, 17]; so we only use the first order model in this study.

4.2 Estimation method

Given the various uncertainties on the mass measurements, classical least square optimization was not suitable to analyze our data and estimate the parameters of the solubility model. Indeed, uncertainties on the fitted parameters are well defined in least square optimization when measurement errors are random. In the case of quartz microbalance technique, the errors due to pressure and temperature effects are systematic. Moreover, when diffusion and relaxation are coupled, the problem is badly conditioned, i.e. close mass kinetics, m(t), can be obtained with quite different parameters sets. To overcome this difficulty we have used a global optimization method, the "set inversion method" [29]. The aim is to estimate all the parameter sets "p=$(\Delta m_d, R, \tau_d, \tau_r)$" that give kinetics lying between two a priori bounding curves, where $\Delta m_d = |c_0 - c_i|e$.

For each sorption or desorption step, the two bounding curves $\Delta m_{min}(t)$ and $\Delta m_{max}(t)$ are calculated from the upper-bound of the different uncertainties mentioned in the experimental section. The real curve should lie

between these two bounding curves. One example is given in figure 2. Let us note that, since the sense of variation of temperature and pressure effects is known, the error amplitudes are not symmetric.

The optimization method is detailed elsewhere [30, 29, 31, 32, 17] and we just give the main features of the SIVIA algorithm (Set Inversion Via Interval Analysis). First, a large a priori variation domain is chosen for each parameter, leading to an initial box in the parameters space (dimension=4):

$$\begin{aligned} 0.1\,s \;\leq\; & \tau_d & \leq\; & t_{end} \\ 0.1\,s \;\leq\; & \tau_r & \leq\; & 10 \times t_{end} \\ 10^{-8}\,kg/m^2 \;\leq\; & \Delta m_d & \leq\; & \Delta m_{end} \\ 10^{-3} \;\leq\; & R & \leq\; & 1 \end{aligned}$$

where t_{end} is the experiment duration (about $2.10^4 s$) and Δm_{end} the mass variation obtained at the end of the experiment (about $2.10^{-6} kg/m^2$ for a 500 nm thick film).

An iterative procedure divides this initial box into smaller and smaller boxes that are partitioned in feasible, unfeasible and ambiguous boxes. A box is said feasible (unfeasible) if all its quadruplets "p" give kinetics $\Delta m(p,t)$ lying (not lying) between the two bounding curves. Other boxes are said ambiguous. After elimination of the unfeasible boxes and selection of the

feasible ones, the ambiguous boxes are divided into smaller ones and the procedure is repeated until the ambiguous domain is small enough.

This method has the great advantage to give well defined uncertainty domain for the four parameters, without favoring any specific solution. The one dimension projections used in this study give the maximum variation domain for each parameter.

4.3 Mutual diffusion coefficient

Differential sorption and desorption steps have been performed at various activities, for the six copolymers. The figure 3 gives an overview of the domain covered by the experiments, each circle or cross corresponding to an experiment (excluding experiments at 0 Torr). The mass fraction corresponding to the glass transition, estimated from previous experiments and which are in agreement with the Chow and Kelley predictions [33, 34], are also plotted onto the graph. As can be seen, most of the experiments lie in the glassy domain since quartz microbalance is not appropriate to mass determination of soft films. Experimental uncertainties were carefully estimated for each experiment (cf section 2). Depending on the duration of the experiment and on the level of the uncertainties, the SIVIA estimation leads to a bounded estimation of the mutual diffusion coefficient (circle symbol) or only to a

minimal bound (cross symbol).

4.3.1 Variations with solvent content

Figure 4 gives the mutual diffusion coefficient versus the solvent mass fraction for all the copolymers. The results are represented in the following way: The horizontal bar corresponds to the solvent mass fraction covered during the step. The vertical bar corresponds to the feasible domain issued from the set inversion method. When only a minimal value of D_{SP} was estimated, no vertical bar is plotted. For the various copolymers, the mutual diffusion coefficient D_{SP} decreases strongly as the solvent concentration decreases: about two orders of magnitude for a 0.05 change in ω_S. Contradictory results have been reported in the literature. Indeed, a same type of behavior has been observed by Boom and Sanoupoulou on the system PMMA/methylacetate [9]. On the contrary, Billovits and Durning had observed a large difference in the variations in the rubbery and glassy domains, finding a nearly constant diffusion coefficient in the glassy domain for the system PS/ethylbenzene [3]. Sun have also obtained a plateau in the glassy domain for the system PHEMA/water [10]. This plateau was interpreted as the consequence of large slow down in free volume decreasing due to the glass transition.

To go deeper in the analysis of these results, further lights are obtained

by analyzing the variation of the mutual diffusion coefficient with copolymer composition on one hand, and by rescaling the results versus " $\omega_S - \omega_{Sg}$ " on the other hand.

4.3.2 Variations with the copolymer composition

The influence of the copolymer composition is analyzed by considering the variation of the mutual diffusion coefficient with the composition, for a given solvent mass fraction. Results are given in Figure 5 for ω_S=0.06 and 0.035. For the two homopolymers (PMMA and PnBMA), only minimum values of D_{SP} have been estimated and they are marked by square. As can be seen, the mutual diffusion coefficient decreases by three or more orders of magnitude when the MMA proportion increases from 0% to 100%. This variation is linear in a semi-log representation that means that the variation of D_{SP} with copolymer composition is exponential, which is consistent with the assumption of additivity of the free volumes. Let us note that this exponential variation with composition is important for practical applications since a slight change in copolymers composition enables to strongly modify the drying kinetics.

4.3.3 Variations with the gap to glass transition

To focus on the glass transition we have plotted the mutual diffusion coefficient versus " $\omega_S - \omega_{Sg}$ ". This representation is similar to the representation in $T - T_g$ used when studying the glass transition induced by temperature. In the concentration range considered in this paper, Kelley and Chow predictions give a conversion factor close for the six polymers: typically a difference on $\omega_S - \omega_{Sg}$ of 0.02 corresponds to a temperature difference $T - T_g$ of about 10^oC. As can be seen by comparing Figures 4 and 6, this representation gathers the results along a master domain, highlighting the prevailing part of the gap to glass transition in the system under study.

It is interesting to compare this master domain to the free volume model frequently used in the literature to express the evolution of Dsp with concentration [35, 36]. We have used the following approach: the parameters that feature in the free volume model developed for rubbery solutions were obtained from the literature for PMMA, PnBMA and Toluene (cf Table 2, [37, 21, 38, 39, 40]). Some dispersion appear in the literature for these parameters and we have compared the prediction deduced from different data set. The interaction parameter ξ was not given in [40] for the system PnBMA/Toluene and we have used the same value than for PMMA/Toluene:

ξ=0.54. No fitting was made, except for the pre-factor. Some examples of the predictions of the free volume model are given in figure 7. Despite the dispersion of the theoretical results, the decreasing of Dsp with the solvent concentration is qualitatively well described by this model whose validity is only established in the rubbery domain. That means that, for the system under study, the diffusion coefficient variation below the glass transition is not deeply modified and that a large slow down in free volume decrease is not observed unlike in [3] and [10].

4.4 Relaxation

This study being mainly focused on diffusion, measurement durations were not long enough to get accurate results on relaxation. However, several comments can be made by looking at the relaxation times estimated by the SIVIA algorithm (Figure 8):

- First, a relaxation term was needed to fit the data for all the performed experiments. Non fickian behavior is observed in the glassy state, as expected, but also just above the glass transition. The lower bound of τ_r is most often greater than the upper bound of the characteristic diffusion time τ_d, which confirms that diffusion is predominant at short times while relaxation dominates at the end of the experiment duration.

- When they are bounded, the obtained values are rather smaller than values reported in the literature for other system (about 10^5 s for PHEMA/water [41] or PMMA/methyl acetate [9], 5.10^2 to 5.10^5 s for PS/ethylbenzene [3, 42]). However, one can wonder about the true meaning of the estimated relaxation times. First, the validity of a description involving only one time of relaxation is not obvious since it is known that relaxation phenomena occurring in the glassy state involve many relaxation modes. That is why a previous study was performed, using a stretched exponential expression to describe relaxation times distribution [17]. It showed that the information brought by the experimental data was not rich enough to estimate accurately the mean relaxation time of the stretched exponential, even if the exponent β is imposed. In the one order model, the estimated relaxation time then probably only reflects phenomena occurring at time scales of the order of the experiment duration. This is confirmed by comparing the estimated relaxation times to the duration of experiments: as can be seen on Figure 8, the maximal bound of τ_r is often close to the experimental duration.

5 Conclusion

A detailed analysis of differential sorption and desorption kinetics have been performed for four copolymers P(MMA/nBMA) and the two homopolymers

P(MMA) and P(nBMA) in the glassy domain. The gravimetric experiments were performed with a quartz microbalance on thin films (about 200 nm to 1000 nm thick). For each experiment, the experimental procedure consists in a preliminary stay at high pressure (in the rubbery domain) to erase the film history. The pressure is then lowered to the initial pressure of the sorption step and maintained a few hours. Then the measurement is performed by applying two successive differential steps (a sorption one and a desorption one). The coupling between diffusion and relaxation was taken into account through the time-dependent solubility model. This model depends on four parameters, describing characteristic times and mass uptakes due to diffusion and relaxation. Given the experimental uncertainties and the coupling between the two phenomena, a global estimation method was developed to get a reliable determination of the four parameters.

Contrary to some authors, we do not observe a large slowing down in the variations of the diffusion coefficient in the glassy state: D_{SP} strongly decreases, of about two orders of magnitude for a 0.05 decrease in ω_S. Results are qualitatively consistent with the free volume model developed for the rubbery domain, showing that, for the system under study, there is no great reduction in the free volume decrease when crossing the glass transition. The

evolution of the mutual diffusion coefficient with the copolymer composition, for a given solvent mass fraction exhibits an increase by three or four orders of magnitude when the MMA proportion decreases from 100% to 0%. An exponential variation with copolymer composition is observed, corresponding to the assumption of additivity of free volumes. An interesting light is obtained by plotting the mutual diffusion coefficient versus $\omega_S - \omega_{Sg}$. In this representation results are gathered along a master domain, highlighting the prevailing part of the gap to glass transition.

These results show that the influence of the glass transition on the diffusion coefficient is a complex problem, involving the physico-chemistry of the system and the distance to the glass transition. Other phenomena have also to be taken into account as the whole thermal and mechanical history of the film, the influence of free or supported films... Further experimental and theoretical studies are needed to improve the understanding of solvent diffusion in the glassy state.

Acknowledgments

The authors gratefully thank Diethelm Johannsmann for having received A.C.Dubreuil in the Max Planck Institute of Polymer Science of Mainz. This work was supported by PEFE (Pechiney Emballage Flexible Europe). The

numerical calculations have been performed on the computers of the "Centre National de Calcul" of CNRS (IDRIS), and of the "Centre de Calcul Recherche" of the University Pierre et Marie Curie (Paris).

References

[1] Enscore, D.; Hopfenberg, H.; Stannett, V.; Berens, A. *Polymer* **1977**, *18*, 1105–1110.

[2] Windle, A. *Journal of Membrane Science* **1984**, *18*, 87–97.

[3] Billovits, G.; Durning, C. *Macromolecules* **1994**, *27*, 7630–7644.

[4] Sanopoulou, M.; Roussis, P.; Petropoulos, J. *J. Polym. Sci.* **1995**, *33*, 993–1005.

[5] Sanopoulou, M.; Roussis, P.; Petropoulos, J. *J. Polym. Sci.* **1995**, *33*, 2125–2136.

[6] Rossi, G.; Pincus, P.; De Gennes, P. *Europhys. Lett.* **1995**, *32*(5), 391–396.

[7] Aminabhavi, T.; Phayde, H. *J. Appl. Polym. Sci.* **1995**, *57*, 1419–1428.

[8] Durning, C.; Hassan, M.; Tong, H.; Lee, K. *Macromolecules* **1995**, *28*, 4234–4248.

[9] Boom, J.; Sanopoulou, M. *Polymer* **2000**, *41*, 8641–8648.

[10] Sun, Y.; Lee, H. *Polymer* **1996**, *37*(17), 3915–3919.

[11] Saby-Dubreuil, A.-C.; Guerrier, B.; Allain, C.; Johannsmann, D. *Polymer* **2001**, *42*, 1383–1391.

[12] Fernandez-Martin, F.; Fernandez-Pierola, I. *J. Polym. Sci.* **1981**, *19*, 1353–1363.

[13] Shetter, J. *Polymer Letters* **1963**, *1*, 209–213.

[14] Penzel, E.; Rieger, J.; Schneider, H. *Polymer* **1997**, *38*(2), 325–337.

[15] Saby-Dubreuil, A.-C. *Séchage de films polymères : Etude du couplage entre la diffusion et la transition vitreuse - Application à des copolymères PMMA/PnBMA* PhD thesis, de l'université Paris VI, **2001**.

[16] Bouchard, C.; Guerrier, B.; Allain, C.; Laschitsch, A.; Saby, A.-C.; Johannsmann, D. *J. Appl. Polym. Sci.* **1998**, *69*, 2235–2246.

[17] Dubreuil, A.-C.; Doumenc, F.; Guerrier, B.; Johannsmann, D.; Allain, C. *Polymer* **2003**, *44*, 377–387.

[18] Lu, C.; Czanderna, A. *Applications of piezoelectric quartz crystal microbalances;* Elsevier, Amsterdam, 1984.

[19] Sanopoulou, M.; Petropoulos, J. *Macromolecules* **2001**, *34*, 1400–1410.

[20] Thomas, N.; Windle, A. *Polymer* **1982**, *23*, 529–542.

[21] Durning, C. *J. Polym. Sci.* **1985**, *23*, 1831–1855.

[22] Edwards, D.; Cohen, D. *AIChE J.* **1995**, *41*, 2345–2355.

[23] Witelski, T. *J. Polym. Sci. B* **1996**, *34*, 141–150.

[24] Long, F.; Richman, D. *J. Am. Chem. Soc.* **1960**, *82*, 513–519.

[25] Frisch, H. L. *J. Chem. Phys.* **1964**, *41*(12), 3679–3683.

[26] Berens, A.; Hopfenberg, H. *Polymer* **1978**, *19*, 489–496.

[27] Sanopoulou, M.; Petropoulos, J. *Polymer* **1997**, *23*, 5761–5768.

[28] Sanopoulou, M.; Stamatialis, D.; Petropoulos, J. *Macromolecules* **2002**, *35*, 1012–1020.

[29] Walter, E.; Pronzato, L. *Identification of parametric models from experimental data;* Springer-Verlag, London, 1997.

[30] Moore, R. *Mathematics and Computers in Simulation* **1992**, *34*, 113–119.

[31] Jaulin, L.; Walter, E. *Mathematics and Computers in Simulation* **1993**, *35*, 123–137.

[32] Jaulin, L.; Walter, E. *Automatica* **1993**, *29*(4), 1053–1064.

[33] Kelley, F.; Bueche, F. *J. Polym. Sci.* **1961**, *L*, 549–556.

[34] Chow, T. *Macromolecules* **1980**, *13*, 362–364.

[35] Vrentas, J.; Duda, J.; Ling, H. *J. Polym. Sci.* **1985**, *23*, 275–288.

[36] Duda, J.; Zielinski, J. *Diffusion in polymers (edited by P.neogi) - Chapter Free-Volume Theory;* Marcel Dekker, Inc, 1996.

[37] Ju, S.; Liu, H.; Duda, J.; Vrentas, J. *J. Appl. Polym. Sci.* **1981**, *26*, 3735.

[38] Ehlich, D.; Sillescu, H. *Macromolecules* **1990**, *23*, 1600–1610.

[39] Zielinski, J.; Duda, J. *AIChE. J.* **1992**, *38*(3), 405.

[40] Tonge, M.; Gilbert, R. *Polymer* **2001**, *42*, 1393–1405.

[41] Sun, Y. *Polymer* **1996**, *37*(17), 3921–3928.

[42] Huang, S.; Durning, C. *J. Polym. Sci. B* **1997**, *35*, 2103–2119.

		PMMA	PMMA/PnBMA copolymers				PnBMA
			I	II	III	IV	
composition			84/16	64/36	48/52	28/72	
tacticity	mm (%)	1	3	5	7	10	2
	mr (%)	25	42	38	38	35	30
	rr (%)	74	55	57	55	55	68
M_n (kg/mol)		220	91	107	207	208	219
$D = M_w / M_n$		1.17	2.93	3.03	2.34	1.41	1.45
T_{g0} (°C)		131	96	75*	63	49	34
ΔC_{pp} (J/K/g)		0.24	0.28	0.24	0.27	0.24	0.30

Table 1: Molecular characteristics (copolymer composition in monomer, tacticity, molar mass M_n, polydispersity D and calorimetric characteristics (glass transition temperature T_{g0}, ΔC_{pp}).
* extrapolated value from Penzel and al. [14].

	PMMA [21]	PMMA [38]	PnBMA [40]
$\widehat{V}_p^*$ (m^3/kg)	$7.89{\cdot}10^{-4}$	$7.89{\cdot}10^{-4}$	$7.88{\cdot}10^{-4}$
$\frac{K_{sp}}{\gamma}$ ($m^3.kg^{-1}.K^{-1}$)	$2.89{\cdot}10^{-7}$	$4.97{\cdot}10^{-7}$	$2.08{\cdot}10^{-7}$
$K_{pp} - T_{gp}$ (K)	- 301	- 342	-137.4
	Toluene [39]	Toluene [37]	
$\widehat{V}_s^*$ (m^3/kg)	$9.17{\cdot}10^{-4}$	$9.17{\cdot}10^{-4}$	
$\frac{K_{ss}}{\gamma}$ ($m^3.kg^{-1}.K^{-1}$)	$1.45{\cdot}10^{-6}$	$2.21{\cdot}10^{-6}$	
$K_{ps} - T_{gs}$ (K)	- 86.32	- 103	

Table 2: Data set obtained in the literature for free volume parameters: $\widehat{V}_s^*$ and $\widehat{V}_p^*$ are the specific hole free volume of solvent and polymer required for a jump, T_{gs} and T_{gp} are the glass transition temperature of solvent and polymer, K_{ss} and K_{sp} denote free-volume parameters for the solvent while K_{ps} and K_{pp} are free-volume parameters for the polymer, γ represents an average overlap factor for the mixture (for more details on the parameters definition, cf for example [36]).

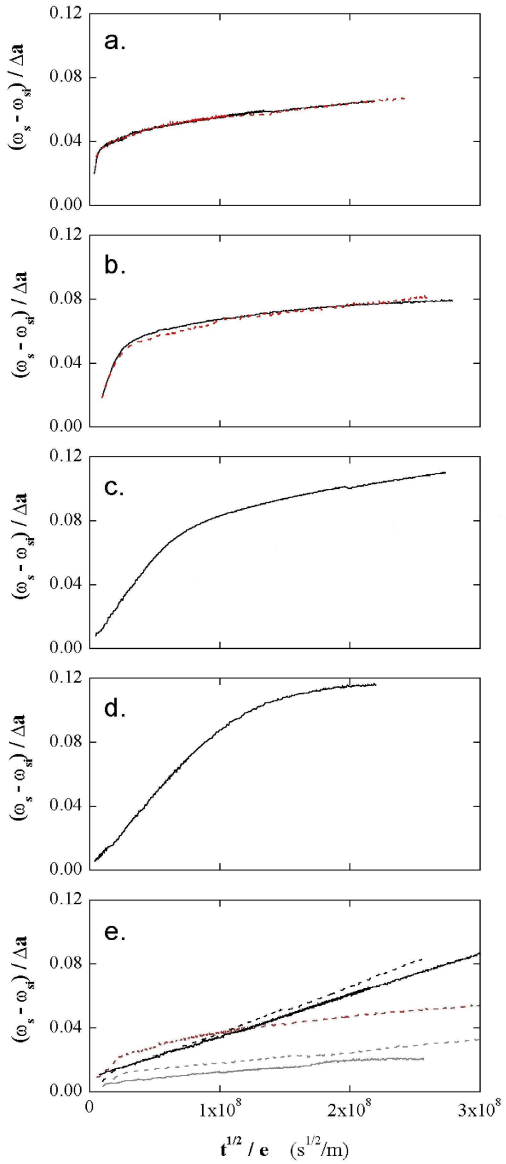

Figure 1: Experimental kinetics obtained for various pressure steps with the 84/16 PMMA/PnBMA copolymer. From top to bottom: (a) Sorption step "8 - 9.7 Torr" (——) and desorption step "9.7 - 8.8 Torr" (- - -). (b) Sorption step "5 - 6.5 Torr" (——) and desorption step "6.5 - 5.9 Torr" (- - -) (Shift from linear mass to cubic mass for $t^{1/2}/e = 10^8\ s^{1/2}/m$) (c) Sorption step "3 -5 Torr" (——) (d) Sorption step "1.8 - 2.5 Torr" (——) (e) Sorption and desorption kinetics obtained for various pressure steps from and towards "zero pressure"- from top to bottom at $t^{1/2}/e = 2 \times 10^8\ s^{1/2}/m$: desorption step "1.2 - 0 Torr", sorption step "0 - 1.2 Torr", desorption step "1.2 - 0 Torr", desorption step "1.2 - 0 Torr" just after annealing, sorption step "1.2 - 0 Torr" just after annealing.

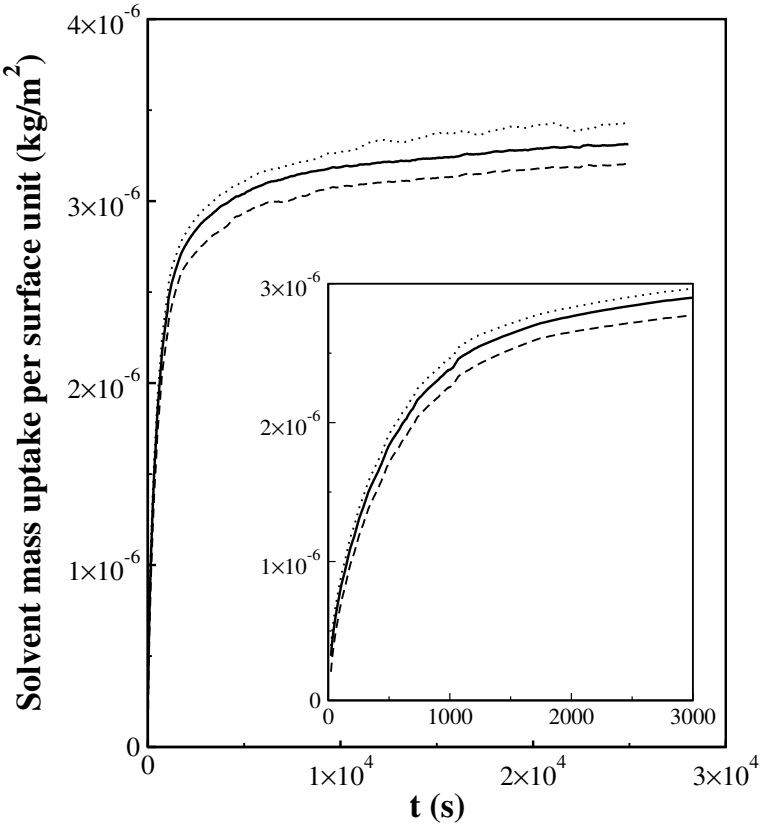

Figure 2: Evolution of the solvent mass per unit surface during the "0.8 - 1.5 Torr" sorption step (copolymer PMMA/PnBMA 48/52, film thickness=400nm). The experimental kinetics $\Delta m(t)$ (——) is surrounded by two curves, the lower bound $\Delta m_{min}(t)$ (- - -) and the upper bound $\Delta m_{max}(t)$ (. . .), calculated taking into account the various uncertainties described in section 2.2. Inset: detail of the evolution at small times.

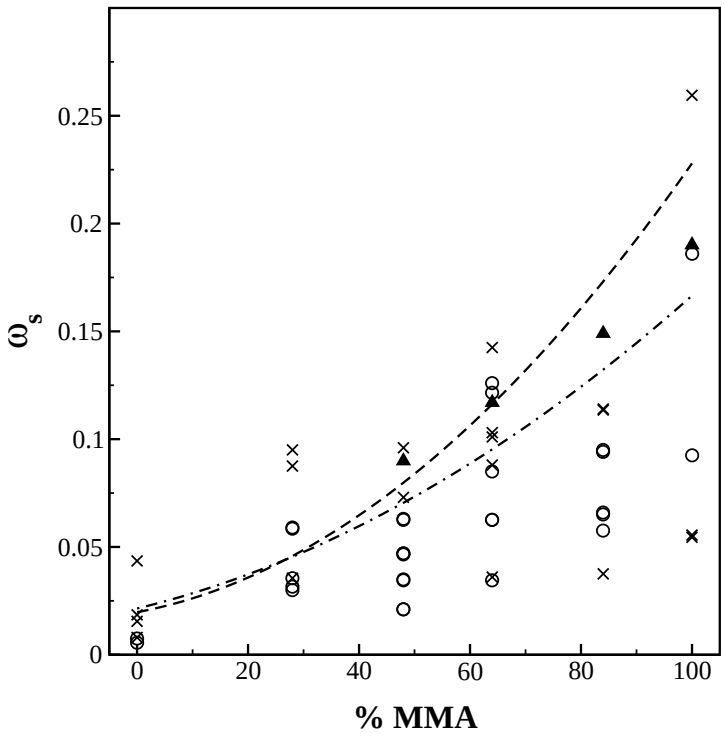

Figure 3: Set of the experiments performed for the estimation of D_{SP}. The circle symbols correspond to experiments giving a bounded estimation of D_{SP} and the cross symbols to experiments giving a minimal value of D_{SP} only. Solvent mass fractions corresponding to the glass transition are also plotted (full triangles: experimental determination, - - -: Chow model, - . -: Kelley model).

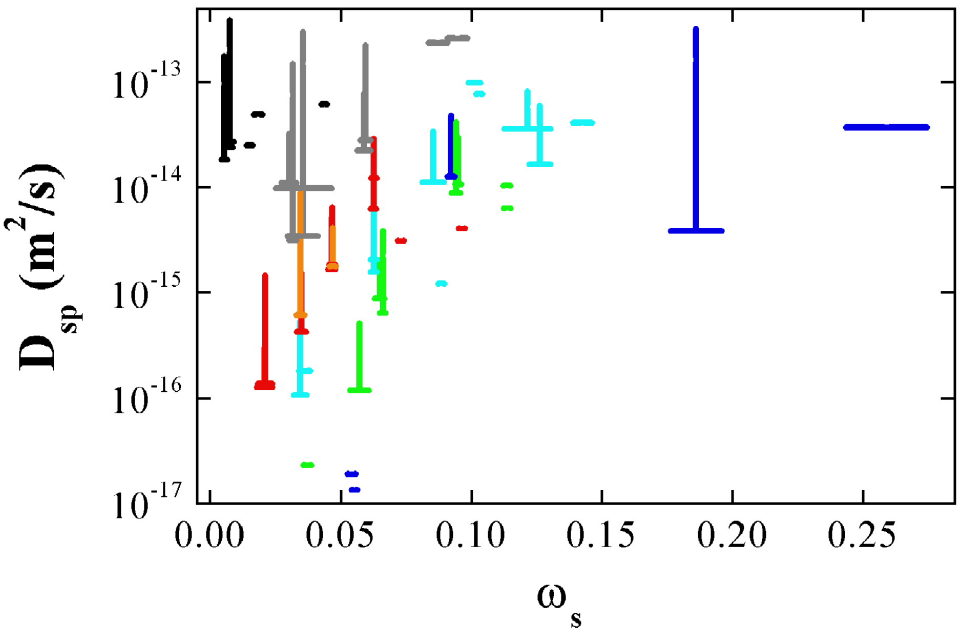

Figure 4: Variation of the mutual diffusion coefficient D_{SP} with the solvent mass fraction ω_S, for all the polymers; PMMA (dark blue), 84/16 (green), 64/36 (light blue), 48/52 (440nm:red, 1100nm:orange), 28/72 (grey), PnBMA (black). Vertical bars correspond to the feasible domain issued from the set inversion method. No vertical bar is drawn when only a minimal values of D_{SP} is known.

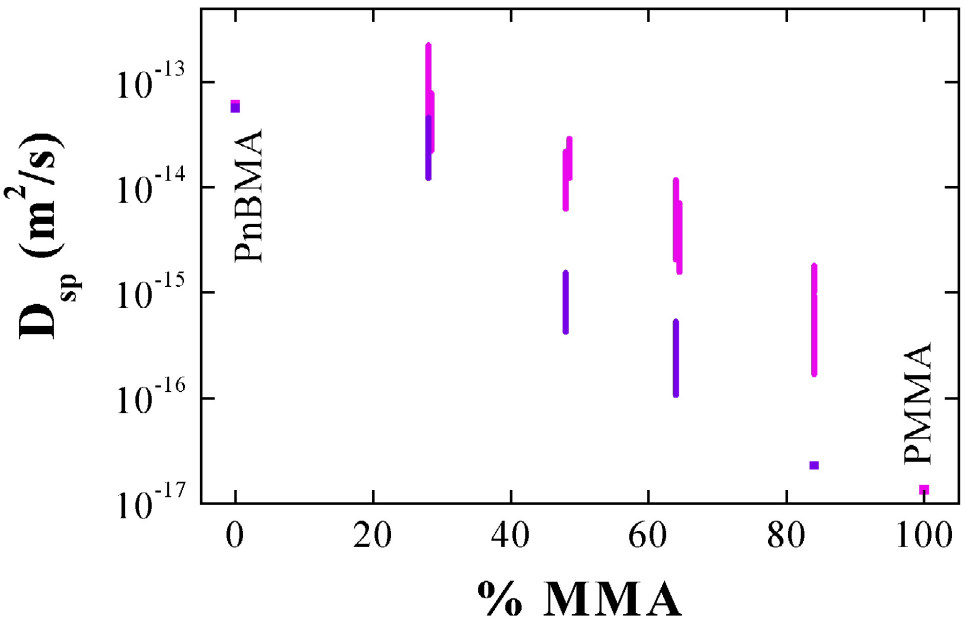

Figure 5: Variation of the mutual diffusion coefficient D_{SP} with the copolymer composition, for $\omega_S = 0.035$ (violet) and $\omega_S = 0.060$ (magenta). Vertical bars correspond to the feasible domain issued from the set inversion method. No vertical bar is drawn when only a minimal values of D_{SP} is known.

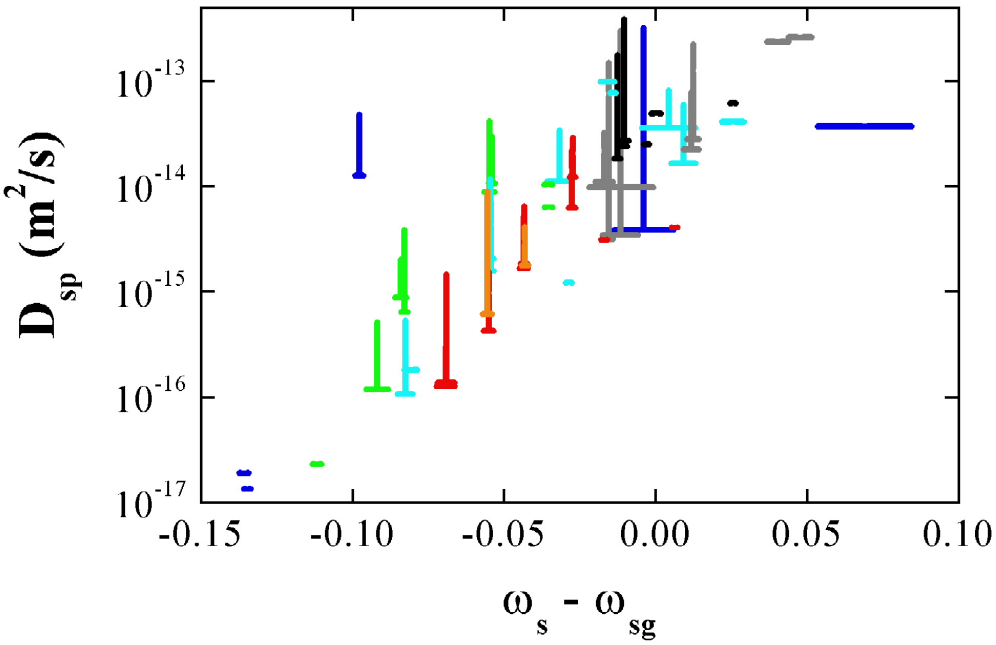

Figure 6: Variation of the mutual diffusion coefficient D_{SP} with $\omega_S - \omega_{Sg}$, for all the polymers; the symbols and colors are the same as in Figure 4.

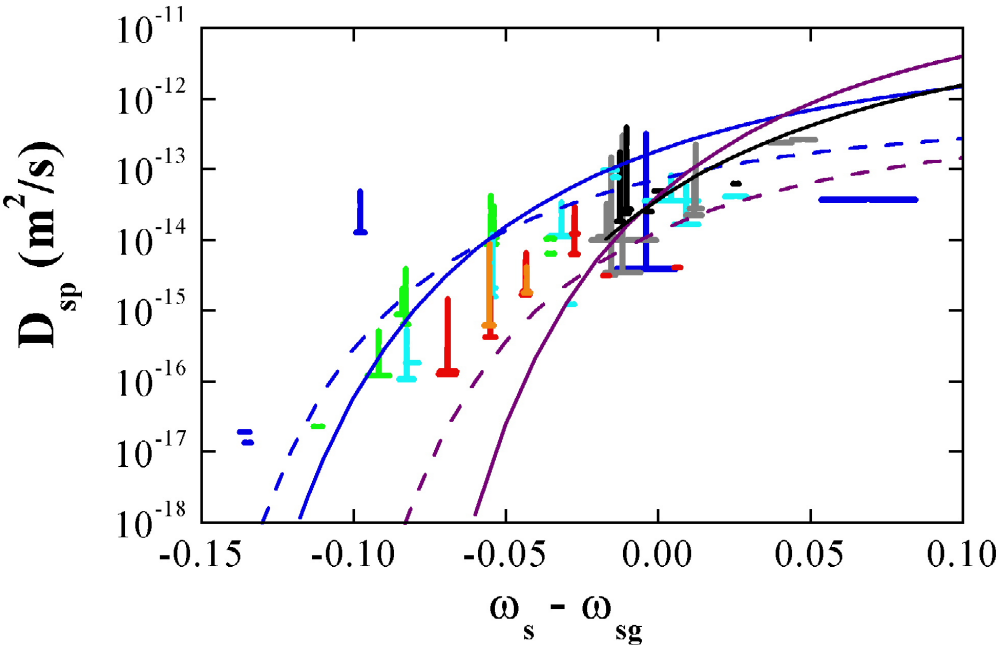

Figure 7: Comparison of the experimental results with the free volume model (see table 2): blue line: toluene [39], PMMA [21], D_{0s} fitted to $3.5 \cdot 10^{-9} m^2/s$, purple line: toluene [39], PMMA [38], $D_{0s} = 3.5 \cdot 10^{-8}\, m^2/s$ [38], blue dotted line: toluene [37], PMMA [21], D_{0s} fitted to $10^{-10}\, m^2/s$, purple dotted line: toluene [37], PMMA [38], D_{0s} fitted to $10^{-10}\, m^2/s$, dark line: toluene [39], PnBMA [40], D_{0s} fitted to $3.5 \cdot 10^{-9}\, m^2/s$.

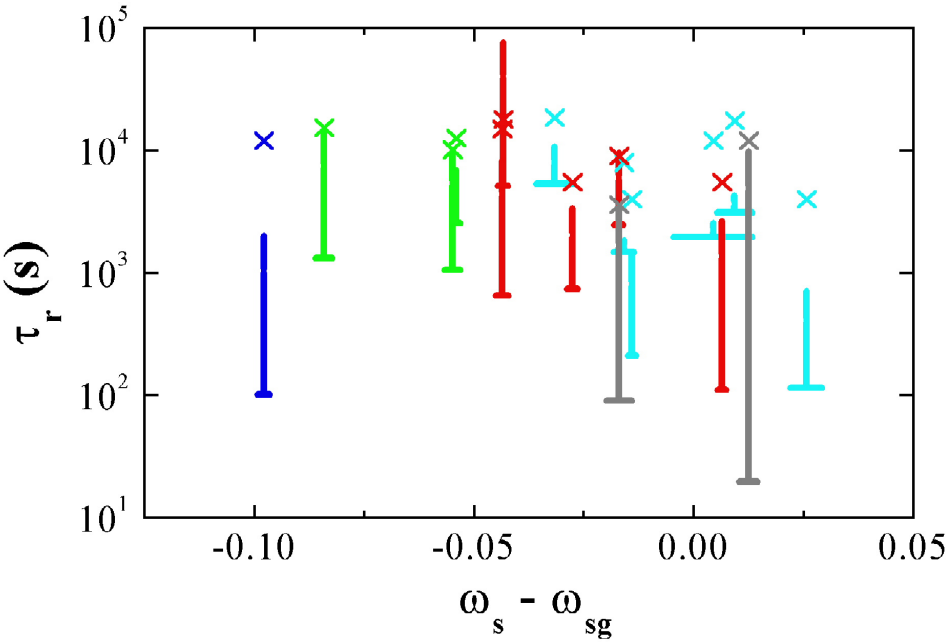

Figure 8: Variation of the relaxation time τ_r with $\omega_S - \omega_{Sg}$ for all the polymers; the colors are the same as in Figure 4. The cross symbols correspond to the duration of the experiments.